HHS Public Access

Author manuscript

*Lab Invest*. Author manuscript; available in PMC 2019 November 16.

Published in final edited form as:

*Lab Invest*. 2019 July ; 99(7): 1030–1040. doi:10.1038/s41374-019-0260-7.

# N-terminal sequences in Matrin 3 mediate phase separation into droplet-like structures that recruit TDP43 variants lacking RNA binding elements

**M. Carolina Gallego-Iradi**[1,2], **Haley Strunk**[1], **Anthony M. Crown**[1,3], **Rachel Davila**[1], **Hilda Brown**[1], **Edgardo Rodriguez-Lebron**[4], **David R. Borchelt**[1]

[1]Department of Neuroscience, Center for Translational Research in Neurodegenerative Disease, McKnight Brain Institute, University of Florida, Gainesville, FL.

[2]present affiliation: Pediatric Stem Cell Transplantation and Regenerative Medicine, School of Medicine, Stanford University, Palo Alto, CA.

[3]present affiliation: Department of Neuroscience, Brown University, Providence, RI.

[4]Department of Pharmacology and Therapeutics, Center for Translational Research in Neurodegenerative Disease, McKnight Brain Institute, University of Florida, Gainesville, FL.

## Abstract

RNA binding proteins associated with amyotrophic lateral sclerosis (ALS) and muscle myopathy possess sequence elements that are low in complexity, or bear resemblance to yeast prion domains. These sequence elements appear to mediate phase separation into liquid-like membraneless organelles. Using fusion proteins of MATR3 to yellow fluorescent protein (YFP), we recently observed that deletion of the second RNA recognition motif (RRM2) caused the protein to phase separate and form intranuclear liquid-like droplets. Here, we use fusion constructs of MATR3, TARDBP43 (TDP43) and FUS with YFP or mCherry to examine phase-separation and protein co-localization in mouse C2C12 myoblast cells. We observed that the N-terminal 397 amino acids of MATR3 (tagged with a nuclear localization signal and expressed as a fusion protein with YFP) formed droplet-like structures within nuclei. Introduction of the myopathic S85C mutation into NLS-N397 MATR3:YFP, but not ALS mutations F115C or P154S, inhibited droplet formation. Further, we analyzed interactions between variants of MATR3 lacking RRM2 (ΔRRM2) and variants of TDP43 with disabling mutations in its RRM1 domain (deletion or mutation). We observed that MATR3:YFP ΔRRM2 formed droplets that appeared to recruit the TDP43 RRM1 mutants. Further, co-expression of the NLS-397 MATR3:YFP construct with a construct that



Address correspondence to David R. Borchelt, 1275 Center Dr., Box 100159, Gainesville, FL 32610, drb1@ufl.edu.

Author Contributions

MCGI: investigation, methodology, visualization, writing-original draft; RD: investigation; AMC: resources; HB: supervision, resources; ER: conceptualization, writing – review & editing, resources; DRB: conceptualization, supervision, writing - review & editing.

Disclosure/Conflict of Interest

The authors have no conflict of interest to declare. Dr. Edgardo Rodriguez-Lebron has recently taken a position with Lacerta Therapeutics (Gainesville, FL, USA), which had no financial contribution to this study and has no financial interests in the outcomes of the study.

encodes the prion-like domain of TDBP43 produced intranuclear droplet-like structures containing both proteins. Collectively, our studies show that N-terminal sequences in MATR3 can mediate phase separation into intranuclear droplet-like structures that can recruit TDP43 under conditions of low RNA binding.

## Introduction

A dominantly inherited mutation in *MATR3* (S85C) was first described in a large, multigenerational family, with slowly progressing (15 years) asymmetrical myopathy and concomitant vocal cord paralysis[1]. Years later, mutations in *MATR3* (F115C, P154S, and T622A) were discovered by exome sequencing in patients with classic ALS[2]. Two of these ALS associated mutations (F115C and T622A) were found in multi-generational families, whereas the P154S mutation was found in a single case of sporadic ALS[2]. The identification of MATR3 mutations in ALS cases, prompted some reconsideration of whether patients with the S85C mutation may have ALS, but other studies have confirmed the S85C mutation as causing myopathy[3–5]. Notably, a number of additional mutations have been found in patients with ALS (total 13), but all of these newer mutations appear to be isolated cases of sporadic disease[6–10].

The 847 amino acid sequence of MATR3 contains multiple recognizable motifs including a nuclear localization signal (NLS), two C2H2-type zinc finger (ZnF) binding domains, and 2 RNA recognition motifs (RRM1 and RRM2)[11,12]. The two RNA binding domains in MATR3 resemble those found in the heterogeneous nuclear ribonucleoproteins (HNRNPs) L and I[12], with RRM2 appearing to be the major RNA binding motif[13]. In prior studies, deletion of RRM2 within MATR3 was found to cause the protein to form intranuclear droplet-like structures[14,15]. In live cell imaging studies, these droplet-like structures were observed to undergo fusion and increase in size as one would observe droplets of water to fuse[14]. This observed property is similar to what is observed *in vitro* for proteins that undergo liquid-liquid phase separation[16].

FUS, TDP43, HNRNPA1 and HNRNPA2B1, which have all also been associated with ALS, share a common sequence motif that is similar to a motif in yeast proteins that display prion-like properties[17]. These prion-like (PrL) domains appear to be critical in enabling these proteins to undergo liquid-liquid phase separation to form membraneless organelles, such as cytoplasmic stress granules[16,18,19]. Mutations in HNRNPA1 and HNRNPA2B1 more commonly cause a type of myopathy called inclusion body myopathy with Paget's disease (with frontotemporal dementia)[17]. MATR3 lacks sequences similar to PrL domains, but large portions of the protein sequence have been described as intrinsically disordered[20], which is a characteristic shared with many other proteins that have been localized to proteinaceous membrane-less organelles that behave as phase-separated liquid-like droplets[21–27].

In the present study, we demonstrate that the N-terminal 397 amino acids of MATR3 are highly prone to produce structures that resemble droplets formed in liquid-liquid phase separation. Mutations in MATR3 associated exclusively with familial ALS (F115C and P154S) had little impact on the ability of MATR3 derivatives to form the droplet structures,

whereas the myopathy-linked S85C mutation largely inhibited droplet formation. MATR3 N-terminal-derived droplets could recruit a co-expressed recombinant C-terminal fragment of TDP43 (encoding its PrL domain) but recruitment of a co-expressed PrL domain of FUS was limited. Collectively, our data identify a sequence element in MATR3 that appears to be able to mediate liquid-liquid phase separation and interactions with TDP43.

## Materials and Methods

### Cloning of vector plasmids

*MATR3* cDNA was obtained from Thermo Scientific (catalog number MHS6278–202757255; Waltham, MA, USA). PCR was performed using this cDNA as template with engineered primers that enabled cloning into a version of the pEF-BOS vector[28] using the InFusion HD kit from Clontech (catalog number 639649, Mountain View, CA). The resulting plasmid was used as the template for PCR with engineered primers to delete the stop codon and allow fusing the YFP to the C-terminus of MATR3 in the pEF-BOS vector, using the InFusion HD kit. Flag- MATR3 del RRM1 (plasmid #32881) and Flag- MATR3 delRRM2 (plasmid #32882) vectors were obtained commercially from Addgene (Cambridge, MA, USA). cDNAs inserts from these plasmids were amplified by PCR, excluding the Flag tag, and cloned into a pEF-BOS.MATR3:YFP vector by swapping out MATR3 cDNA sequences, using the Infusion HD kit. BOS-MATR3:YFPΔRRM2-S85C and F115C were generated by site directed mutagenesis with a QuickChange II XL kit (catalog #200521, Agilent Technologies, Santa Clara, CA). Similarly, MATR3:YFP-RRM1-M and MATR3:YFP-RRM2-M constructs were generated by QuickChange to introduce V400D/H402D mutations in RRM1 or V498D/H500D/S502D mutations in RRM2, respectively.

BOS-TDP43-mCher was produced by PCR amplification of the coding sequences for TDP43 (Addgene plasmid #28206) and amplification of the cDNA for mCherry (from pEZ-M56 Cat #EX-P0037, Gene-Copoeia, Rockville, MD, USA), followed by insertion into a vector termed CTR0 [gift of Dr. Todd Golde, described in[29]]. The TDP43:mCher fusion cDNA was then inserted into the pEF.BOS vector using an InFusion HD kit. The BOS-TDP43-ΔRRM1 construct was produced by deleting aa 106–175 by PCR mutagenesis and the BOS-TDP43-RRM1-M construct was created by mutating amino acids 106–111 from LIVLGL to DIDLGD[30]. The cDNA constructs for these genes were inserted into pEF.BOS using the InFusion kit.

The N-terminal 397-MATR3 constructs were generated by PCR amplification using primers designed to enable in-frame fusion to YFP at the C-terminus. For the NLS-397-MATR3:YFP construct, the 5’ primer used in PCR amplification was modified to encode a consensus start codon and a consensus NLS sequence (ccaccATGcctccaaaaaagaagagaaaggtagacgtc, which translates to (Kozak)-MPPKKKRKVDV) that would be fused in-frame to the coding sequence for the N-terminal 397 amino acids of MATR3. The BOS-NLS-C263TDP43:mCher construct was generated by PCR using 5’ primers modified to encode a consensus start codon followed by a consensus NLS sequence, same as above, to produce an amplicon in which the codons for the C-terminal 263 amino would be in-frame. The BOS-NLS-N284-FUS:mCher construct was made by first amplifying the N-terminal 284 amino acids of FUS and separately amplifying

mCherry by PCR using primers engineered to fuse mCherry to the C-terminus of the truncated FUS cDNA. These fragments were cloned into pEF-BOS using the InFusion HD kit. The resulting construct was used as template for PCR with a 5' primer designed to contain the same consensus Kozak and NLS sequences described above and cloned into pEF-BOS using the InFusion HD kit. All constructs were verified by DNA sequencing before use.

### Cell lines, transfection and immunohistochemistry

C2C12 mouse myoblasts (ATCC, Manassas, VA) used in transfection experiments were cultured in DMEM Medium from Thermo Scientific (catalog number 11965–084) with 10% fetal bovine serum, 2 mM glutamine, 100 U.I./ml penicillin streptomycin from Thermo Scientific (catalog number 15140122) and 2ug/ml Fungizone from Gemini Bioproducts (catalog number 400–104). Cells were cultured at 37°C and 5% $CO_2$. Cells were seeded at $25\times10^4$ densities in log-phase growth 24 h before transfection in to glass coverslips that had been coated with poly-lysine. Lipofectamine 3000 (Invitrogen, Carlsbad, CA) was used for transient transfection following manufacturer protocols. Cells where incubated in lipofectamine with a total of 1.5 μg of DNA per well. After transfection, the cells were switched to DMEM medium with 2% horse serum, 2 mM glutamine, 100 U.I./ml penicillin streptomycin and 2 μg/ml Fungizone to induce myoblast differentiation. Each transfection was repeated at least three times and each transfection was performed in duplicate. MATR3 and TDP43 cotransfections were performed at a 1:1 ratio of expression vectors for each.

### Microscopy

Cells plated on glass coverslips were washed twice with PBS and fixed with 4% paraformaldehyde for 10 minutes. After fixation, the coverslips were washed 3 times in PBS and then treated with Vectashield Antifade mounting medium (Vector Laboratories, Burlingame, CA). Microscopy was performed using three different microscopes depending upon the type of analysis required. In some cases, we used an Olympus BX60 epifluorescence microscope fitted with a color camera to capture images. For some experiments, we used an Olympus FV1000/DSU-IX81 Spinning Disc Confocal microscope, controlled by Slidebook software (v4.2, Intelligent Imaging Innovations, Inc, Denver, CO). Images captured by either of these microscopes were cropped and prepared for presentation with Photoshop (CS6 version 13.0.1 × 64, Adobe Systems Incorporated, San Jose, CA). In a few cases, we used a laser-scanning confocal microscope Nikon A1RMP image system with a Nikon A1R scanner, Nikon A1-DUG 4 channel filter based detector unit and Nikon LUNV Laser Launch (6 lines) with a 40x objective, or a 60x water immersion objective. The excitation/emission wavelengths during acquisition were 488 nm/492–557 nm for GFP. Images were processed using Nikon NIS-Elements software v4.5 (Nikon Instruments, Inc., Melville, NY).

## Results

In previous work, WT and mutant MATR3 expressed as either untagged proteins, or as fusion proteins with YFP, were observed to be primarily localized to the nucleus where they displayed a diffuse distribution with discernable puncta[31]. In the present study, we have

focused almost exclusively on examining WT and mutant MATR3 behavior in mouse C2C12 myoblasts. At least one mutation in MATR3 has been associated with myopathy[1,3], and we have recently discovered that expression of the F115C variant of MATR3 in mouse muscle can cause pathological changes associated with myopathy[32]. To study MATR3 localization in C2C12 cells, we have expressed human MATR3 fused to YFP. Similar to what was observed in other cell types, WT and mutant MATR3 were primarily localized to the nucleus of C2C12 myoblasts (Fig. 1; Supplemental Fig. S1). We used a paradigm of transient transfection, where it is common to observe a range of expression levels within the same dish. In a small subset of cells (estimated to be <5%) that were exceptionally fluorescent, a portion of the expressed MATR3:YFP was localized in puncta scattered within the cytosol; however, in the vast majority of the cells the fluorescence was exclusively nuclear. In comparing cells with higher levels of fluorescence to adjacent cells with lower levels, we observed that in cells with low levels of expression there was an obvious granular texture to the appearance of the protein (Fig 1A and B, inset). At higher levels of expression, we observed the emergence of brighter puncta, but the overall granular appearance was preserved (Fig 1C and D, inset). Cells expressing MATR3:YFP with the F115C mutation showed nuclear localization and texture that was similar to cells expressing WT MATR3:YFP (Fig. 1E–H). Similar to WT MATR3, a subset of highly fluorescent cells expressing F115C MATR3:YFP also showed evidence of cytoplasmic puncta (Fig. 1E and F, inset).

In a recent proteomic study of the MATR3 interactome, we observed that deletion of the RRM2 element in MATR3 caused a dramatic change in the appearance of the protein within nuclei with more subtle changes in appearance by deletion of RRM1[14]. MATR3:YFP constructs lacking RRM1 produced a globular distribution of the protein within nuclei, whereas deletion of RRM2 produced a protein that was organized into spherical structures that resemble droplets (Fig. 2)[14]. Notably, cells containing the MATR3:YFPΔRRM2 droplets show altered distribution of chromatin, with the droplets appearing to exclude DNA stained by Dapi (Fig. 2G and H, arrow marks one example).

A large number of nuclear proteins possess the capability of undergoing liquid-liquid phase separation to assemble into distinct nuclear substructures[27]. Although a subset of these carry glycine rich sequence elements that are similar to yeast prion domains, most of them have domains characterized as intrinsically disordered (Supplemental Fig. S2). The N-terminal 397 and the C-terminal 276 amino acids of MATR3 exhibit low sequence complexity and are predicted to be disordered (Supplemental Fig. S2). Initially, we focused on characterizing the larger N-terminal sequence by expressing YFP-fusions in muscle-derived C2C12 cells. MATR3 encodes multiple sequence elements with similarity to nuclear localization signals (NLS), including the sequence KRRR located at residues 146–150[15]. A recent study mapped the primary functional NLS in full-length MATR3 to the sequence KKDKSRKRSYSPDGKESPSDKKSK between amino acids 588 and 611[15]. Notably, in cells expressing N397-MATR3:YFP, the fluorescent spherical structures were primarily intranuclear with extranuclear structures appearing at a lower frequency (Supplemental Fig. S3). To ensure targeting of the N397 construct to the nucleus, the predominant location of WT MATR3, we fused a canonical NLS sequence (MPPKKKRKVDV) to the N-terminus of the construct. In cells expressing NLS-N397-MATR3:YFP, all of the fluorescent protein was

nuclear and organized into spherical droplet-like structures that were dispersed throughout the nucleus (Fig. 3). Introduction of the S85C mutation into the NLS-N397-MATR3:YFP construct largely inhibited droplet formation compared to WT-N397-MATR3:YFP (Fig. 4A, B, E and F). By contrast, the F115C and P154S mutations appeared to have little impact on droplet formation (Fig. 4). Thus, the N-terminal sequence of MATR3 appears to be able to undergo phase separation to form liquid-like droplets, or it can readily integrate into a yet to be defined pre-existing nuclear compartment. Intriguingly, the S85C mutation, which is associated with myopathy, inhibited or destabilized coalescence into these structures.

Previous studies have reported that MATR3 can interact with TDP43[2]; however, we have observed limited co-localization of WT MATR3:YFP and WT TDP43:mCher when co-expressed in mouse C2C12 cells[14]. Recent studies have shown that TDP43 will undergo phase separation to form liquid-like droplets *in vitro*[16] and that fusion constructs of GFP-TDP43 with a disabled RNA binding domain (RRM1) can produce intranuclear droplet structures when over-expressed in HEK293 cells[22]. Intranuclear droplets of GFP-TDP43 were observed by deletion of RRM1, missense mutation of RRM1 (RRM1-M as previously described[30]), or by replacement of RRM1 with sequences for GFP[22]. In prior studies, we had built TDP43 fusions with C-terminal mCherry and here we deleted or mutated RRM1 to create two constructs, TDP43:mCherRRM1-M, which encodes missense mutations in the RNA binding site, and TDP43:mCherΔRRM1, which deletes amino acids 106 to175. When either of these constructs were expressed, alone, the fusion proteins were predominantly localized to the nucleus and appeared to be distributed in a manner similar to WT TDP43:mCher (Supplemental Fig. S4). Presumably, the location of the fluorescent tag influenced the ability of these TDP43 fusion proteins to produce droplet structures. To determine whether TDP43 with a disabled RRM1 domain may be drawn into droplets formed by MATR3:YFPΔRRM2, we co-expressed the constructs in mouse C2C12 myoblasts where we observed droplets containing both proteins (Fig. 5A and B). When we co-expressed F115C MATR3:YFPΔRRM2 with TDP43:mCherRRM1-M, we observed that a portion of the TDP43 protein was co-localized with the droplets formed by the F115C mutant (Fig. 5C). From these types of transient co-transfection experiments, it is difficult to determine whether the MATR3:YFP construct with the F115C mutation is quantifiably less able to intermingle with TDP43-mCherRRM1-M. A more obvious outcome was observed when the S85C variant of MATR3:YFPΔRRM2 was co-expressed with TDP43:mCherRRM1-M, where the presence of the S85C mutation disrupted droplet formation and droplets containing TDP43:mCherRRM1-M were also lacking (Fig. 5D). As previously reported[14], we observed minimal co-localization of WT TDP43:mCher in droplets formed by MATR3:YFPΔRRM2 (Fig. 5E). These data suggest that there may be circumstances related to the binding of nucleic acids by RRM1 of TDP43 that potentiate interactions between MATR3 and TDP43, and that the S85C mutation may disrupt such interactions.

To determine whether the interactions between TDP43 and MATR3 may involve their low complexity domains, we produced a construct in which the PrL domain of TDP43 (C-terminal 263 amino acids) was fused to mCherry (C263-TDP43:mCher). We modified it to include an N-terminal nuclear localization signal (NLS-C263-TDP43:mCher) and co-expressed it with NLS-N397-MATR3:YFP. As expected, the NLS-N397-MATR3:YFP

construct produced droplet like structures (Fig. 6A). In cells co-expressing the two constructs a portion of NLS-C263-TDP43:mCher resided within the droplets formed by NLS-N397-MATR3WT:YFP (Fig. 6B). When expressed alone, the NLS-C263-TDP43:mCher construct did not generate droplet-like structures (Fig. 6C). To ask whether any PrL domain from any related protein would co-localize to MATR3 droplet structures, we generated a recombinant construct of the FUS PrL domain (N-terminal 284 amino acids) fused to mCherry with an N-terminal NLS (NLS-N284-FUS:mCher) for expression with our MATR3 construct. In this case, we did not observe the obvious droplets of NLS-N284-FUS:mCher co-localizing with NLS-N397-MATR3:YFP droplets; however, much smaller and fainter spheres of NLS-N284-FUS:mCher fluorescence were visible (Fig. 6D–F). Collectively, these findings imply that sequence elements within the N-terminal 397 amino acids of MATR3 and the C-terminal PrL domain of TDP43 are capable of interacting in a somewhat specific manner. These interactions seem more prone to occur when MATR3 is induced to produce droplet-like structures.

## Discussion

We demonstrate that the 397 amino acid N-terminal segment of MATR3, which lacks RNA binding domains and has been described as intrinsically disordered[20], is prone to produce liquid-like droplet structures in the nucleus when over-expressed. Mutations in this segment that cause ALS do not produce obvious changes in droplet morphology or location, but cells expressing MATR3 constructs that included the S85C mutation, which causes distal myopathy, lacked droplet structures. We also investigated potential interactions between MATR3 and TDP43 that could occur within these liquid-like droplets. Prior studies have demonstrated that interactions between full-length WT MATR3 and TDP43 can occur[2,14,33,34]. Although the level of interaction between full-length MATR3 and TDP43 proteins has been reported to be relatively weak[14], our data suggests that there could be circumstances in which more robust interactions occur. Specifically, we demonstrate that MATR3 constructs that are capable of forming liquid-like droplets will recruit TDP43 carrying a disabled RRM1 domain or expressed fragments of TDP43 that encompass the PrL domain. Collectively, our studies suggest that circumstances that diminish nucleic acid binding to the RRM2 of MATR3 and the RRM1 of TDP43 could allow these proteins to comingle in some type of liquid-like compartment.

The low complexity domains of RNA binding proteins that are found in liquid-like membraneless organelles appear to be essential in phase separation[35]. The PrL domains of TDP43, FUS, HNRNPA1, and HNRNPA2B1 are typically very Gly rich and low in charged residues (see Fig. S2). Many proteins that are found in stable intranuclear proteinaceous membraneless organelles lack the PrL domain homology and, instead, are characterized as intrinsically disordered[27]. Examples of such proteins include SRSF4 (nuclear speckles), SAFB (nuclear stress bodies), and RBMX (Sam68 nuclear bodies), which like MATR3, can bind RNA through RRM domains (Fig. S2). The low complexity domains of these proteins are Arg/Ser, or Arg/Gly rich and contain a high number of charged residues (more positively than negatively charged) (Fig. S2). Other proteins found in stable intranuclear liquid-like structures include SMN (Gem bodies), NOLC1 (Cajal bodies), SOX9 (paraspeckles), and CBP (PML bodies)[27]. The disordered elements of these proteins have varied compositions

though they are generally rich in two or three amino acids (e.g. Pro/Ser, Gln/Pro/Ser, and Gln/Pro/Gly) and with varying amounts of charged residues (Fig. S2). The N-terminal 397 amino acids of MATR3 upstream of RRM1 (aa 1–397) and the segment of the protein downstream of RRM2 (aa 572 – 8471) have been described as intrinsically disordered[20]. Although not examined here, it is possible that the disordered MATR3 C-terminal segment can also mediate phase separation if expressed as a protein fragment. The N-terminal 397 amino acid segment is modestly enriched for Gly, Leu, and Ser (10, 10, & 12% by composition) and contains an equal number of negatively and positively charged amino acids (49 & 46, respectively) (Supplemental Fig. S5). Embedded within the N-terminal 397 amino acids of MATR3 is a Zn finger domain (amino acids 291–320). The role that this element could have in phase separation remains to be resolved. It is possible that this element mediates binding to a nucleic acid that participates in the organization of phase separated organelles such as occurs in nuclear paraspeckles[36]. Overall, it is clear that MATR3 shares key features with proteins found in liquid-like intranuclear structures.

Whether the MATR3 constructs we have examined here populate some pre-existing subnuclear compartment or form novel structures has yet to be clarified. In previous work to characterize MATR3 interaction networks, we identified proteins found in the nucleolus and nuclear speckles as MATR3 binding partners[14]. Clearly, however, MATR3 is not normally localized to the nucleolus, and MATR3 has not been described as a common constituent of nuclear speckles[37]. Additionally, the interaction network for MATR3ΔRRM2, which forms droplets, identified a large number of novel protein interactions that were not consistent with any of the well characterized subnuclear membraneless organelles (see Supplemental Table 7 in[14]). Collectively, these findings suggest that over-expression of the N-terminal segment of MATR3, or the RRM2 deletion mutant, may drive self-assembly into novel phase-separated nuclear compartments. The physiologic relevance of these structures has yet to be defined. Moreover, the role of liquid-liquid-phase separation in MATR3 function or disease processes is unknown. We show that the F115C and P154S mutations of ALS do not remarkably alter this property, but the S85C mutation of myopathy appeared to disrupt the formation of stable droplets. It is possible that some change in the ability of MATR3-S85C to phase separate could contribute to myopathic abnormalities by altering a function of MATR3 that is critical in myoblasts. Notably, however, a recent study of transgenic mice that express the F115C variant of MATR3 in muscle demonstrated profound myopathy[32], suggesting that altered ability to phase separate is not inextricably linked to muscle toxicity.

The frequency with which MATR3 may undergo phase separation *in vivo* is unclear. In cells expressing WT or mutant MATR3 at low levels, the protein is primarily localized to the nucleus and distributed diffusely with a granular texture. As the protein is over-expressed, there is some localization to the cytosol and we observe nuclear puncta, but no obvious droplets are visible as might be expected if the level of MATR3 exceeded the level of its normal RNA substrates. Thus, although we are tempted to conclude that the N397-MATR3 and the MATR3ΔRRM2 variants can form droplets due to diminished binding to nucleic acid substrates in the nucleus[38], it is possible that other types of protein:protein interactions involving the RRM2 domain of MATR3 influence phase transition.

Several prior studies have identified TDP43 as an interactor with MATR3[2,14,33,34]. The initial description of mutations in MATR3 in patients with ALS described cell culture co-transfection studies that produced evidence of MATR3:TDP43 interactions[2]. Subsequent proteomic studies using affinity capture paradigms have confirmed MATR3:TDP43 interactions can occur, but these interactions could be described as relatively weak[14]. In prior microscopy studies of MATR3 and TDP43 interaction, relatively little evidence of co-localization of WT or mutant MATR3:YFP and WT TDP43:mCher was observed by confocal imaging[14]. Here, we show sequence elements within MATR3 can mediate phase separation and, within the droplet structures formed, we observe robust co-localization of TDP43 variants with disabled RRM1 domains. The TDP43 C-terminal PrL domains appeared to be more readily incorporated into MATR3 containing droplets than the PrL domain of FUS. Notably, our C-terminal mCher fusion constructs with the PrL domain of TDP43 or FUS did not spontaneously form droplets on their own in the mouse C2C12 cell model. The dependency of droplet formation on MATR3 interaction with TDP43 is further evident in cells co-expressing S85C MATR3 constructs with TDP43 constructs. Collectively, these findings indicate that the N-terminal sequences of MATR3 and C-terminal sequences of TDP43 have a capacity to coalesce into intermingled droplet-like structures. Whether the co-localization of these derivatives of MAT3 and TDP43 is due to direct protein:protein interactions or some other type of co-mingling of proteins in the liquid-like structures that could contain other ribonucleoprotein complexes requires further investigation.

## Conclusions

In summary, our study demonstrates that the N-terminal 397 amino acids of MATR3 expressed as fusion proteins with YFP can mediate localization into liquid-like intranuclear droplets as occurs in phase separation. Two ALS-associated mutations in MATR3 that occur in this N-terminal segment had little impact on droplet formation, but the S85C mutation that causes myopathy was highly disruptive. The conditions in which MATR3 may undergo phase separation at physiologic levels of expression are presently unclear, as structures similar to what we describe here have not been observed in normal mice or in muscle tissues of transgenic mice that express WT or F115C MATR3 at 2 to 3 fold over endogenous levels[32]. It is not surprising that visualizing the large droplets observed here would require over-expression. Determining whether phase separation events on a much smaller scale occur when these proteins are at physiologic levels is very challenging. Our study predicts that if there are circumstances in which MATR3 undergoes phase separation, perhaps when interactions with RNA substrates are diminished, then TDP43 could be recruited to such structures if it also uncoupled from RNA substrates. Understanding how processes related to the capacity of MATR3 and TDP43 to produce liquid-like structures could regulate interactions between these proteins, and how mutations associated with disease affect such interactions, could provide new insight into pathogenic mechanisms in ALS and myopathy.

## Supplementary Material

Refer to Web version on PubMed Central for supplementary material.

## Acknowledgements

This work was supported by funding from the McKnight Brain Institute, the SantaFe HealthCare Alzheimer's Disease Research Center and by shared equipment grant (NIH Grant # 1S10OD020026 – Dr. Habibeh Khoshbouei, PI). We thank Doug Smith and the Cell and Tissue Analysis Core for assistance in this study. We thank Rohan Mangal for help in generating some of the MATR3 constructs. We are grateful to Dr. Jada Lewis for helpful discussion and Pat Joy for help in proofreading.

## References

1. Senderek J et al. Autosomal-dominant distal myopathy associated with a recurrent missense mutation in the gene encoding the nuclear matrix protein, matrin 3. Am. J. Hum. Genet 84, 511–518 (2009). [PubMed: 19344878]
2. Johnson JO et al. Mutations in the Matrin 3 gene cause familial amyotrophic lateral sclerosis. Nat. Neurosci 17, 664–666 (2014). [PubMed: 24686783]
3. Muller TJ et al. Phenotype of matrin-3-related distal myopathy in 16 German patients. Ann. Neurol 76, 669–680 (2014). [PubMed: 25154462]
4. Mensch A et al. The p.S85C-mutation in MATR3 impairs stress granule formation in Matrin-3 myopathy. Exp. Neurol 306, 222–231 (2018). [PubMed: 29763601]
5. Palmio J et al. Re-evaluation of the phenotype caused by the common MATR3 p.Ser85Cys mutation in a new family. J. Neurol. Neurosurg. Psychiatry 87, 448–50 (2016). [PubMed: 25952333]
6. Lin K-P et al. Mutational analysis of MATR3 in Taiwanese patients with amyotrophic lateral sclerosis. Neurobiol. Aging 36, 2005e1–4 (2015). [PubMed: 25085785]
7. Origone P et al. A novel Arg147Trp MATR3 missense mutation in a slowly progressive ALS Italian patient. Amyotroph. Lateral Scler. Frontotemporal Degener 16, 530–531 (2015). [PubMed: 26199109]
8. Leblond CS et al. Replication study of MATR3 in familial and sporadic amyotrophic lateral sclerosis. Neurobiol. Aging 37, 209.e17–209.e21 (2016).
9. Marangi G et al. Matrin 3 variants are frequent in Italian ALS patients. Neurobiol. Aging 49, 218.e1–218.e7 (2017).
10. Purice MD & Taylor JP Linking hnRNP Function to ALS and FTD Pathology. Front. Neurosci 12, 326 (2018). [PubMed: 29867335]
11. Belgrader P, Dey R & Berezney R Molecular cloning of matrin 3. A 125-kilodalton protein of the nuclear matrix contains an extensive acidic domain. J. Biol. Chem 266, 9893–9899 (1991). [PubMed: 2033075]
12. Hibino Y et al. Molecular properties and intracellular localization of rat liver nuclear scaffold protein P130. Biochim. Biophys. Acta 1759, 195–207 (2006). [PubMed: 16814881]
13. Salton M et al. Matrin 3 binds and stabilizes mRNA. PLoS One 6, e23882 (2011). [PubMed: 21858232]
14. Iradi MCG et al. Characterization of gene regulation and protein interaction networks for Matrin 3 encoding mutations linked to amyotrophic lateral sclerosis and myopathy. Sci. Rep 8, 4049 (2018). [PubMed: 29511296]
15. Malik AM et al. Matrin 3-dependent neurotoxicity is modified by nucleic acid binding and nucleocytoplasmic localization. Elife 7, (2018).
16. Molliex A et al. Phase separation by low complexity domains promotes stress granule assembly and drives pathological fibrillization. Cell 163, 123–133 (2015). [PubMed: 26406374]
17. Kim HJ et al. Mutations in prion-like domains in hnRNPA2B1 and hnRNPA1 cause multisystem proteinopathy and ALS. Nature 495, 467–473 (2013). [PubMed: 23455423]
18. Aulas A & Velde C Vande. Alterations in stress granule dynamics driven by TDP-43 and FUS: a link to pathological inclusions in ALS? Front. Cell. Neurosci 9, 423 (2015). [PubMed: 26557057]
19. Patel A et al. A Liquid-to-Solid Phase Transition of the ALS Protein FUS Accelerated by Disease Mutation. Cell 162, 1066–1077 (2015). [PubMed: 26317470]
20. Coelho MB et al. Nuclear matrix protein Matrin3 regulates alternative splicing and forms overlapping regulatory networks with PTB. EMBO J. 34, 653–668 (2015). [PubMed: 25599992]

21. Brangwynne CP et al. Germline P granules are liquid droplets that localize by controlled dissolution/condensation. Science 324, 1729–1732 (2009). [PubMed: 19460965]
22. Schmidt HB & Rohatgi R In Vivo Formation of Vacuolated Multi-phase Compartments Lacking Membranes. Cell Rep. 16, 1228–1236 (2016). [PubMed: 27452472]
23. Thiam AR, Jr RVF & Walther TC The biophysics and cell biology of lipid droplets. Nat. Rev. cell Biol. 14, 775–786 (2013).
24. March ZM, King OD & Shorter J Prion-like domains as epigenetic regulators, scaffolds for subcellular organization, and drivers of neurodegenerative disease. Brain Res. 1647, 9–18 (2016). [PubMed: 26996412]
25. Meng F, Na I, Kurgan L & Uversky VN Compartmentalization and Functionality of Nuclear Disorder: Intrinsic Disorder and Protein-Protein Interactions in Intra-Nuclear Compartments. Int. J. Mol. Sci 17, (2015).
26. Uversky VN, Kuznetsova IM, Turoverov KK & Zaslavsky B Intrinsically disordered proteins as crucial constituents of cellular aqueous two phase systems and coacervates. FEBS Lett. 589, 15–22 (2015). [PubMed: 25436423]
27. Uversky VN Intrinsically disordered proteins in overcrowded milieu: Membrane-less organelles, phase separation, and intrinsic disorder. Curr. Opin. Struct. Biol 44, 18–30 (2016). [PubMed: 27838525]
28. Mizushima S & Nagata S pEF-BOS, a powerful mammalian expression vector. Nucleic Acids Res. 18, 5322 (1990). [PubMed: 1698283]
29. Bean LA et al. Re-Opening the Critical Window for Estrogen Therapy. J. Neurosci 35, 16077–16093 (2015). [PubMed: 26658861]
30. Buratti E & Baralle FE Characterization and functional implications of the RNA binding properties of nuclear factor TDP-43, a novel splicing regulator of CFTR exon 9. J. Biol. Chem 276, 36337–36343 (2001). [PubMed: 11470789]
31. Gallego-Iradi MC et al. Subcellular Localization of Matrin 3 Containing Mutations Associated with ALS and Distal Myopathy. PLoS One 10, e0142144 (2015). [PubMed: 26528920]
32. Moloney C et al. Analysis of spinal and muscle pathology in transgenic mice overexpressing wild-type and ALS-linked mutant MATR3. Acta Neuropathol. Commun 6, 137 (2018). [PubMed: 30563574]
33. Boehringer A et al. ALS Associated Mutations in Matrin 3 Alter Protein-Protein Interactions and Impede mRNA Nuclear Export. Sci. Rep 7, 14529 (2017). [PubMed: 29109432]
34. Ling SC et al. ALS-associated mutations in TDP-43 increase its stability and promote TDP-43 complexes with FUS/TLS. Proc. Natl. Acad. Sci. U. S. A 107, 13318–13323 (2010). [PubMed: 20624952]
35. Guo L & Shorter J It's Raining Liquids: RNA Tunes Viscoelasticity and Dynamics of Membraneless Organelles. Mol. Cell 60, 189–192 (2015). [PubMed: 26474062]
36. Fox AH, Nakagawa S, Hirose T & Bond CS Paraspeckles: Where Long Noncoding RNA Meets Phase Separation. Trends Biochem. Sci 43, 124–135 (2018). [PubMed: 29289458]
37. Mohamad N & Boden M The proteins of intra-nuclear bodies: a data-driven analysis of sequence, interaction and expression. BMC Syst. Biol 4, 44 (2010). [PubMed: 20388198]
38. Maharana S et al. RNA buffers the phase separation behavior of prion-like RNA binding proteins. Science 360, 918–921 (2018). [PubMed: 29650702]

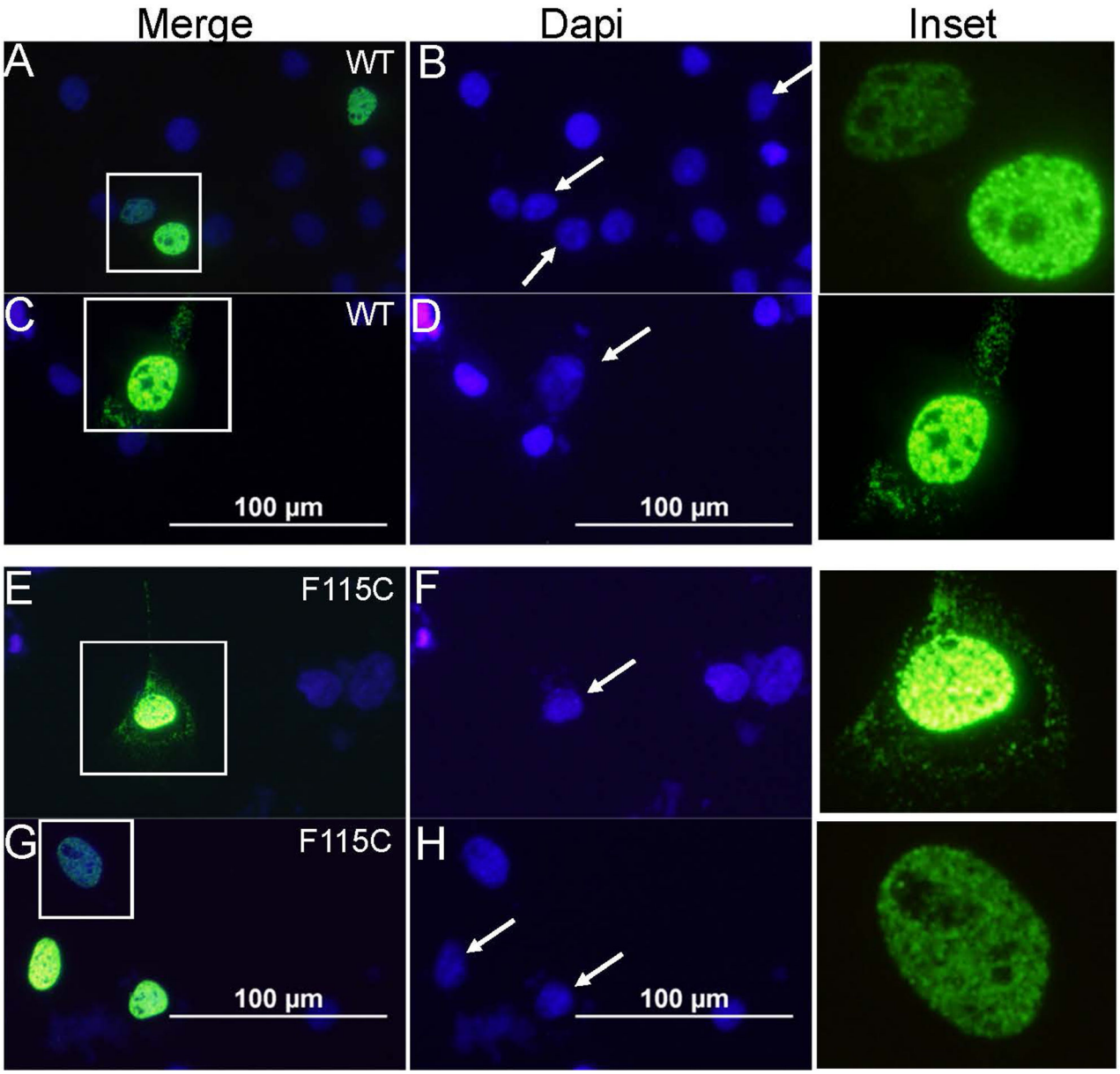


**Fig 1. Effect of over-expression on the distribution of WT and mutant MATR3:YFP in C2C12 cells.**

**A-G** Mouse C2C12 cells were grown on glass cover slips and transiently transfected with pEF.Bos vectors encoding WT (**A-D**) and F115C (**E-H**) MATR3:YFP variants. At 24 hours post-transfection, the cells were fixed and imaged with an Olympus epifluorescence microscope (40x original magnification). The images shown are representative of images seen in 3 independent transfections, viewing at least 50 transfected cells on each cover slip. **A** Image of two cells with different levels of expression with an image of the Dapi channel (**B**) (inset digitally magnified). **C, E** In a subset of highly fluorescent cells, expressing either WT (**C**) or mutant (**E**) MATR3:YFP, fluorescence is visible in the cytosol (insets digitally magnified). Images of these cells in the Dapi channel shown in **D** & **F**, respectively. **G** Image of cells expressing F115C MATR3:YFP at different levels with image from the Dapi

channel (**H**) (inset of lower expressing cell digitally magnified). The arrows in **B, D, F,** & **H** mark the cells that express the YFP fusion proteins at high levels (Dapi only channel).

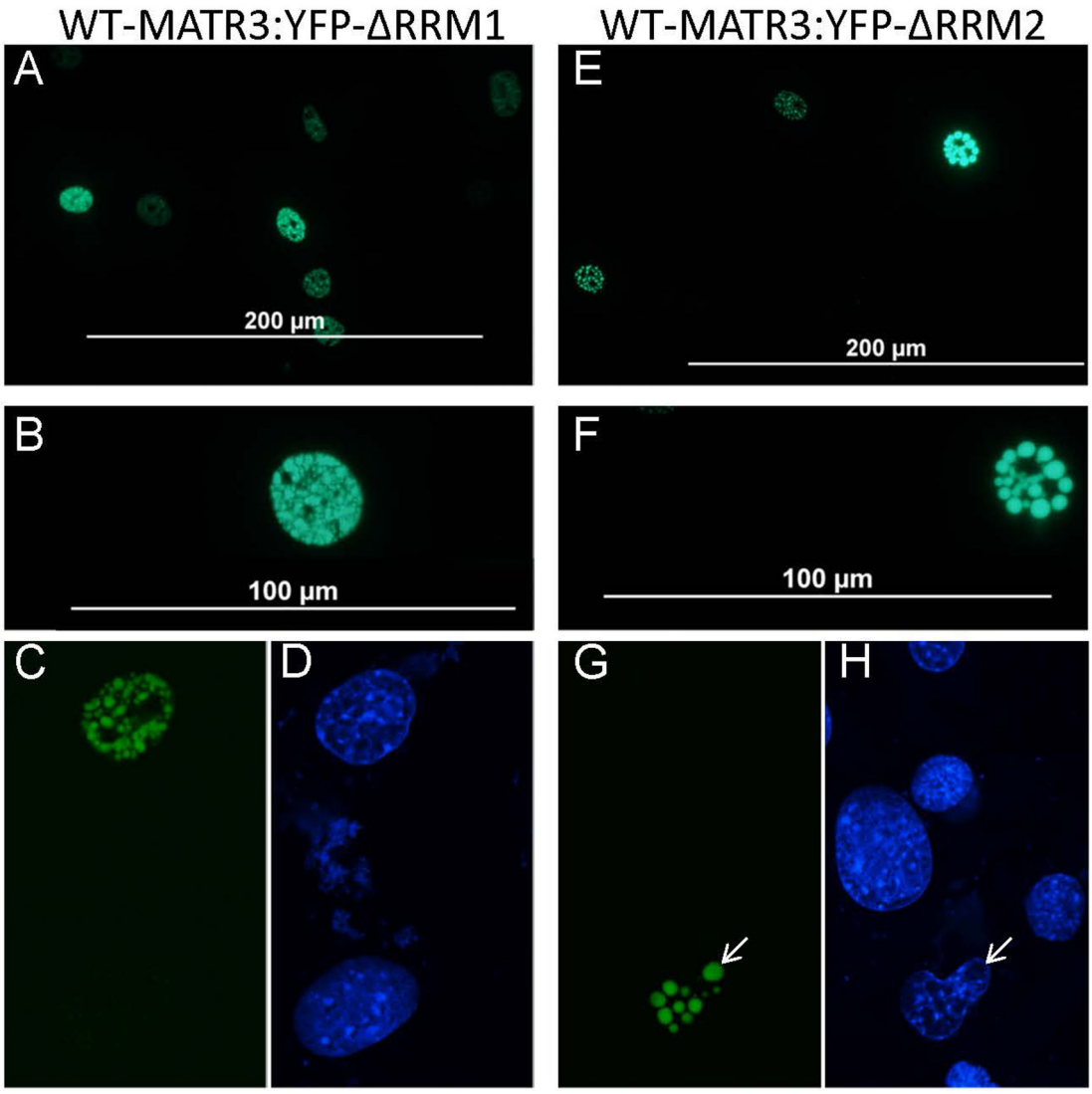


**Fig 2. MATR3:YFP lacking RRM1 or RRM2 displays a greater tendency towards formation of spherical droplet-like intranuclear structures.**

Mouse C2C12 cells were grown on glass cover slips and transiently transfected with pEF.Bos vectors encoding WT MATR3:YFP lacking RRM1 (**A-D**) or RRM2 (**E-H**). At 24 hours post-transfection, the cells were fixed and imaged with an Olympus epifluorescence microscope (40x original magnification). The images shown are representative of images seen in 3 independent transfections, viewing 20 to 40 cells on each cover slip.

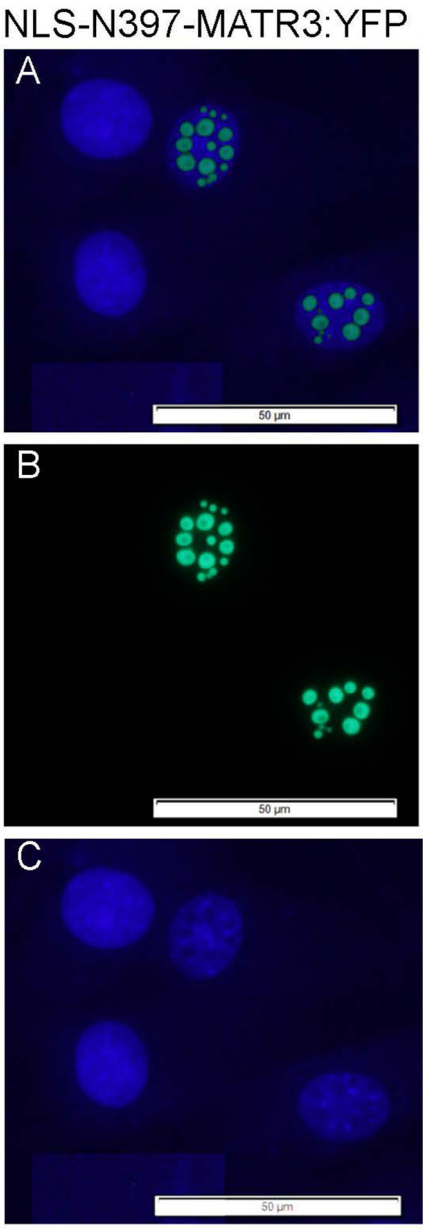


**Fig 3. N-terminal fragments of MATR3 targeted to the nucleus spontaneously form spherical droplet-like structures.**

**A-C** Mouse C2C12 cells were grown on glass cover slips and transiently transfected with pEF.Bos vectors encoding NLS-N397-MATR3:YFP. At 24 hours post-transfection, the cells were fixed and imaged with an Olympus epifluorescence microscope (40x original magnification). The images shown are representative of images seen in 3 independent transfections, viewing at least 50 cells on each cover slip. (**A**) Merged images, (**B**) YFP channel alone, (**C**) Dapi channel alone.

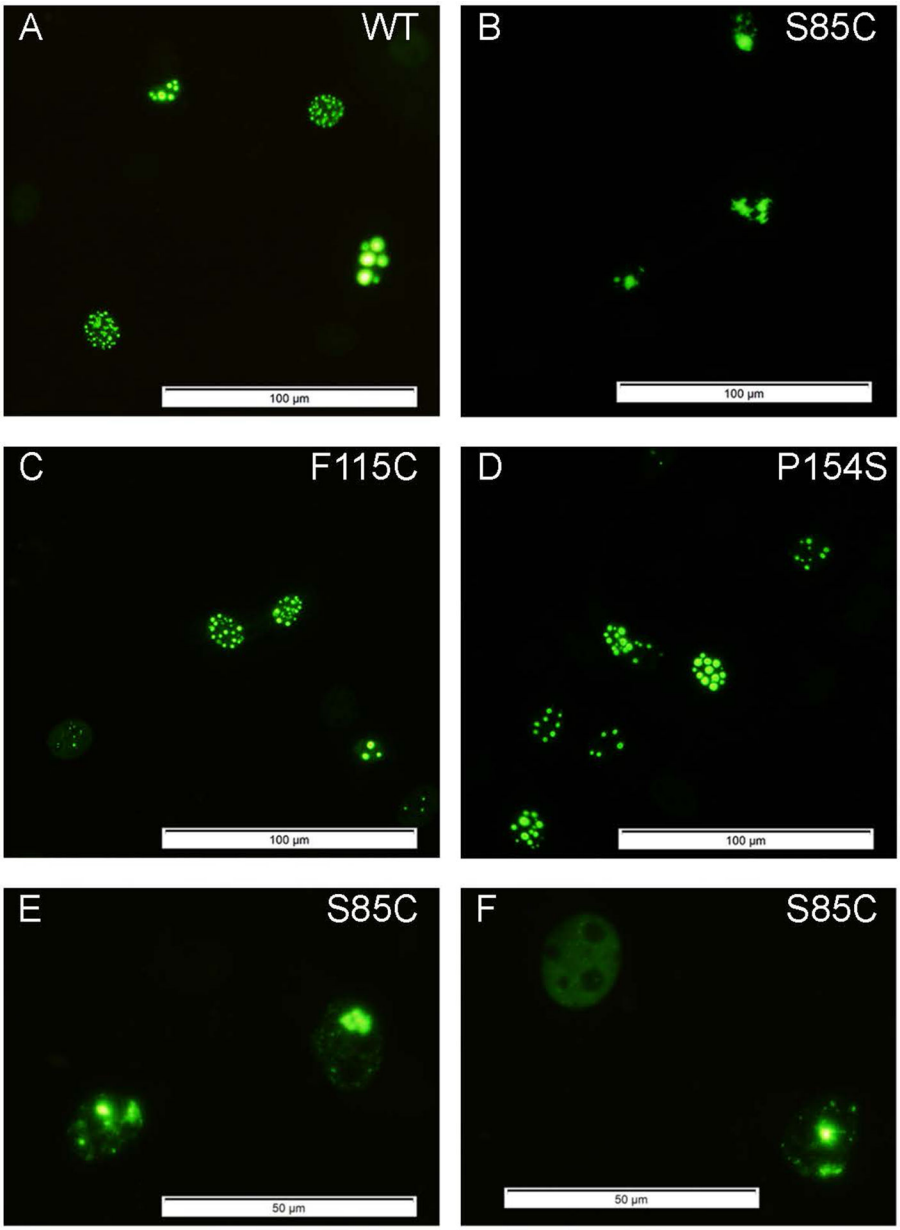


**Fig. 4. Variable effects of disease mutations on the morphology of NLS-N397-MATR3:YFP within the nucleus.**

Mouse C2C12 cells were grown on glass cover slips and transiently transfected with pEF.Bos vectors encoding NLS-N397-MATR3:YFP with the mutations indicated in each panel. At 24 hours post-transfection, the cells were fixed and imaged with an Olympus epifluorescence microscope. **A-D** Images captured at 20x magnification. **E&F** Images captured at 40x magnification. The images shown are representative of images seen in 3 independent transfections, viewing at least 50 cells on each cover slip.

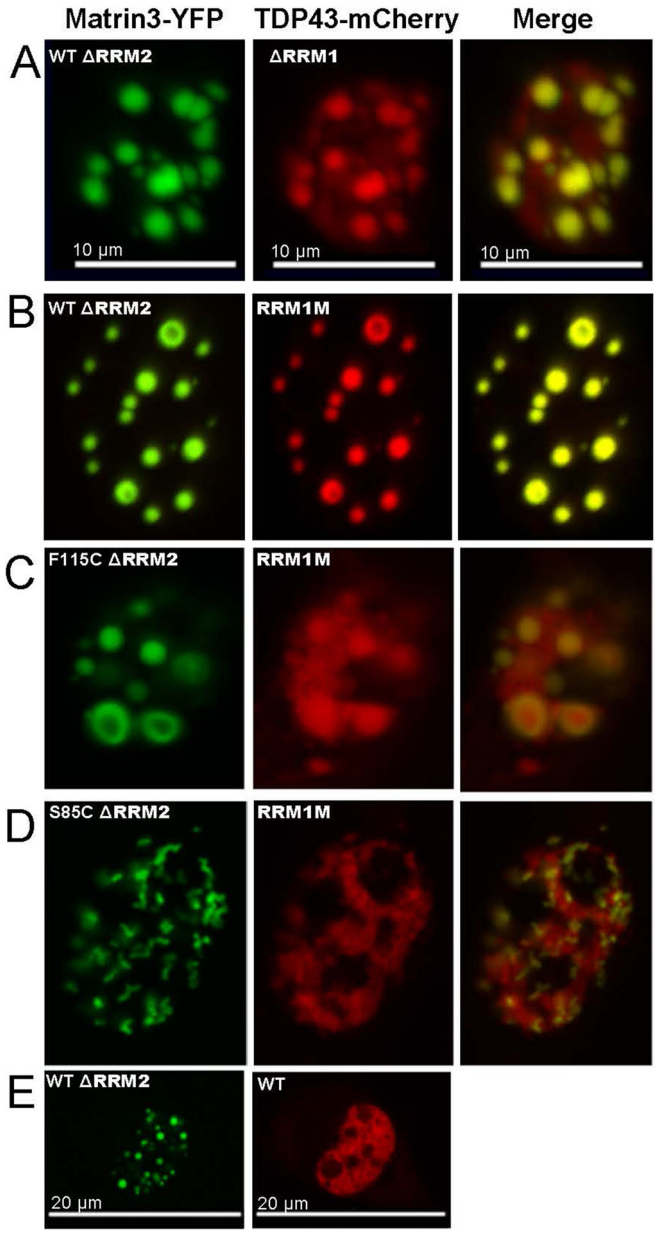


**Fig 5. Co-localization of MATR3:YFP-WT-ΔRRM2 and TDP43:mCherry variants with disabled RRM1 domains.**

Mouse C2C12 cells were co-transfected with MATR3:YFP and TDP43:mCher constructs as indicated below. The images shown are representative of what was found in at least two separate transfection experiments analyzing 50–100 transfected cells in each experiment. **A-D** Images were captured with a Nikon A1RMP imaging system (original magnification 60x with 2x digital enlargement; scale bars are approximations). Each image is from a single z-plane. **A** & **B** WT MATR3:YFPΔRRM co-expressed with TDP43:mCherΔRRM1 or TDP43:mCherRRM1-M. **C** & **D** F115C or S85C MATR3:YFPΔRRM co-expressed with TDP43:mCherRRM1-M. **E** WT MATR3:YFPΔRRM co-expressed with WT TDP43:mCher at original magnification (60X). Expression plasmids were generated as described in Materials and Methods.

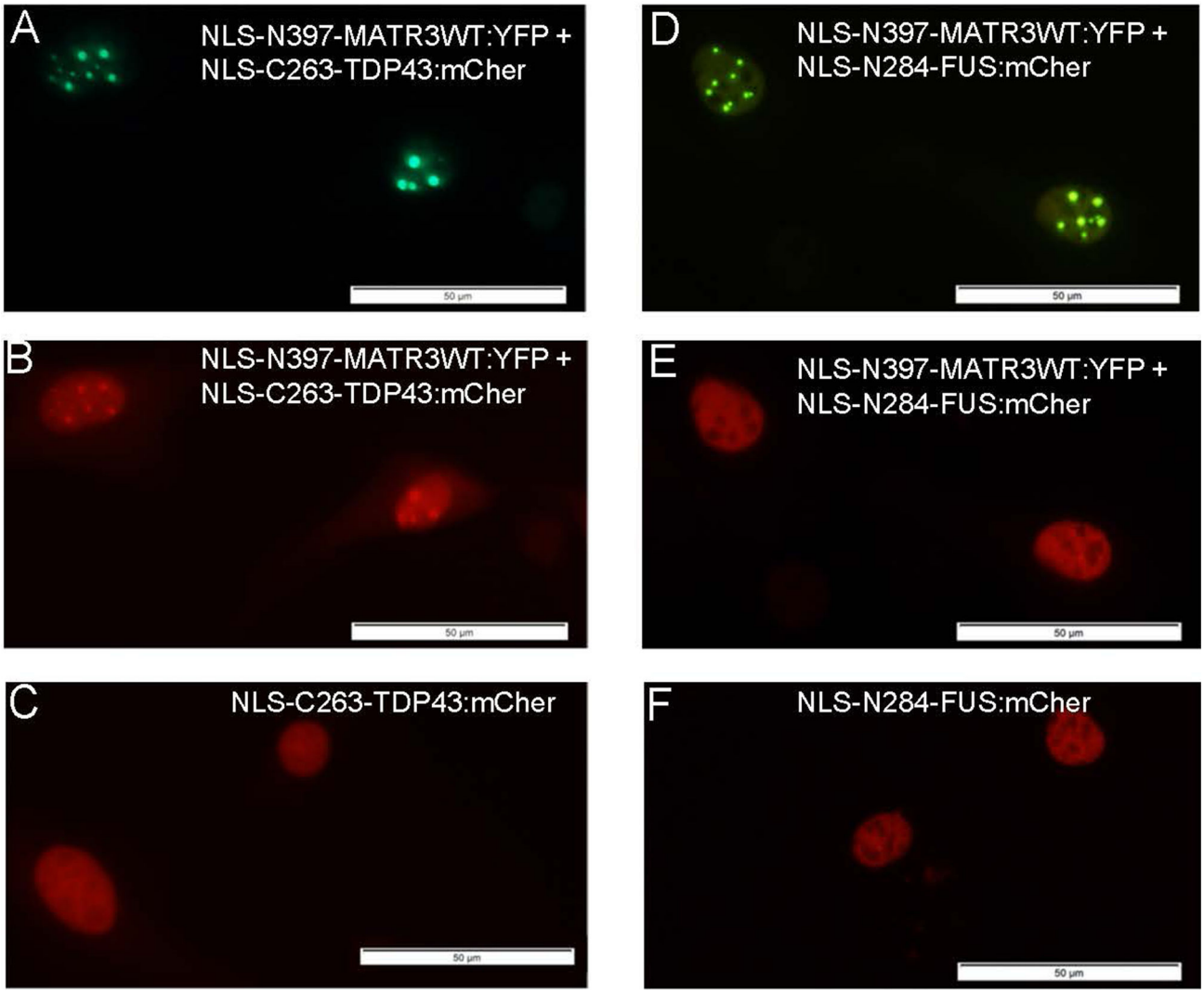


**Fig 6. Co-localization of NLS-N397:MATR3WT:YFP with PrL domain of TDP43 in spherical droplet-like structures.**

**A-B** Mouse C2C12 cells were grown on glass cover slips and transiently co-transfected with pEF.Bos vectors encoding NLS-N397-MATR3:YFP and NLS-C263-TDP43:mCher; **A** shows the YFP channel and **B** shows the mCherry channel. **C** Cells transfected with NLS-C263-TDP43:mCher alone. **D-E** Mouse C2C12 cells co-transfected with NLS-N397-MATR3:YFP and NLS-N284-FUS:mCher; **D** shows the YFP channel and **E** shows the mCher channel. **F** Cells transfected with NLS-N284-FUS:mCher, alone. At 24 hours post-transfection, the cells were fixed and imaged with an Olympus spinning disk confocal microscope (projection images; original magnification 40x). The images shown are representative of images seen in 3 independent transfections, viewing at least 50 cells on each cover slip.